

Supporting Information

Vivid tumor imaging utilizing liposome-carried bi-modal radiotracer

Jonghee Kim,^a Darpan N. Pandya,^a Woonghee Lee,^a Jang Woo Park,^b Youn Ji Kim,^a Wonjung Kwak,^a Yeong Su Ha,^a Yongmin Chang,^{a,b} Gwang Il An^{*c} and Jeongsoo Yoo^{*a}

^a Department of Molecular Medicine, Kyungpook National University, Daegu 700-422, South Korea.

^b Department of Medical & Biological Engineering, Kyungpook National University, Daegu 700-422, South Korea

^c Molecular Imaging Research Center, Korea Institute of Radiological and Medical Sciences, Seoul 139-706, South Korea

Table of Contents

Materials and methods	S3
Instrumentation	S3
Synthesis of hexadecyl-4-iodobenzoate	S4
Synthesis of hexadecyl-4-tributylstannylbenzoate	S6
Radiolabeling of HIB	S8
Preparation of [¹²⁴ I]HIB-Gd-containing liposome	S9
Physicochemical characterization of [¹²⁴ I]HIB-Gd-containing liposome	S10
In vitro imaging study of [¹²⁴ I]HIB-Gd-containing liposome	S11
Determination of Partition Coefficients	S13
Blood half-life measurement of [¹²⁴ I]HIB and [¹²⁴ I]HIB-labeled liposome.....	S12
Animal study	S13
In vivo Optical Imaging	S13
In vivo PET Imaging	S13
In vivo MR Imaging	S14
MR Image Analysis	S14

Materials and methods: 1,2-dipalmitoyl-sn-glycero-3-phosphoethanolamine-N-diethylenetriaminepentaacetic acid (Gd-DTPA-DPPE), 1,2-distearoyl-sn-glycero-3-phosphoethanolamine-N-[methoxy(polyethylene glycol)-2000] (DSPE-mPEG₂₀₀₀) and other lipids were purchased from Avanti Polar lipids (Alabaster, AL, USA). [¹²⁴I]NaI was produced by ¹²⁴Te(p,n)¹²⁴I reaction in the Korea Institute of Radiology and Science (KIRAMS, Seoul, Korea). 1-hexadecanol and other chemicals were purchased from Sigma-Aldrich (St. Louis, MO, USA). PD-10 Desalting column (Sephadex™ G-25 Medium) was purchased from GE Healthcare (Pittsburgh, PA, USA) and Luna C8 HPLC column was purchased from Phenomenex (Torrance, CA, USA).

Instrumentation: All ¹H NMR and ¹³C NMR spectra were measured on Varian Unity Inova 500 MHz instrument. High-resolution mass spectra (HRMS) were recorded on JEOL JMS700 or Quattro Premier XE mass spectrometer. Elemental analyses were carried out at Kyungpook National University, Korea. HPLC traces were acquired using Waters 600 series HPLC system. The radio-TLC measurements were performed using a Bioscan 2000 imaging scanner (Bioscan, Washington, D.C., USA). Size Particle were measured by light scattering with a particle size analyzer (ELS-Z, Zeta potential and particle size analyzer, Otsuka, Japan). The morphology of liposomes were observed using transmission electron microscopy (TEM, HITACHI, Tokyo, Japan). MicroPET image was acquired by small-animal Inveon PET scanner (Siemens). Optical image was acquired by IVIS spectrum (PerkinElmer) and MR image was performed using GE Excite 1.5T scanner (GE Healthcare).

Synthesis of hexadecyl-4-iodobenzoate: 4-iodobenzoyl chloride (1.32 g, 4.94 mmol) was added to a stirred solution of 1-hexadecanol (1.0 g, 4.12 mmol) and triethylamine (1.22 mL, 0.88 g, 8.74 mmol) in CH₂Cl₂ (30 mL). The reaction mixture was stirred at room temperature for 3h. After evaporation of solvent under reduced pressure, 25 mL of 0.1 N HCl was added. The resultant reaction mixture was extracted with CH₂Cl₂ (3 × 30 mL), the combined organic phases were washed by brine, dried over MgSO₄, and concentrated to give yellowish white solid, which was recrystallized in hexane/CH₂Cl₂ to afford white crystalline needles of hexadecyl-4-iodobenzoate (1.42g, 80% yield). ¹H NMR (500 MHz, CDCl₃): δ 0.87-0.89 (t, 3H, *J* = 7 Hz), 1.26 -1.44 (m, 26H), 1.72-1.78 (m, 2H), 4.29-4.31 (t, 2H, *J* = 7 Hz), 7.73-7.75 (dd, 2H, *J* = 8 Hz), 7.78-7.80 (dd, 2H, *J* = 8 Hz); ¹³C NMR (125 MHz, CDCl₃): δ 14.11, 22.68, 25.99, 28.64, 29.25, 29.35, 29.50, 29.56, 29.62, 29.64, 29.66, 29.68, 31.91, 65.39, 100.50, 129.99, 130.98, 137.64, 166.12; HRMS (FAB) calculated for C₂₃H₃₈O₄I, 473.1917 [(M+H)⁺], found: 473.1917[(M+H)⁺].

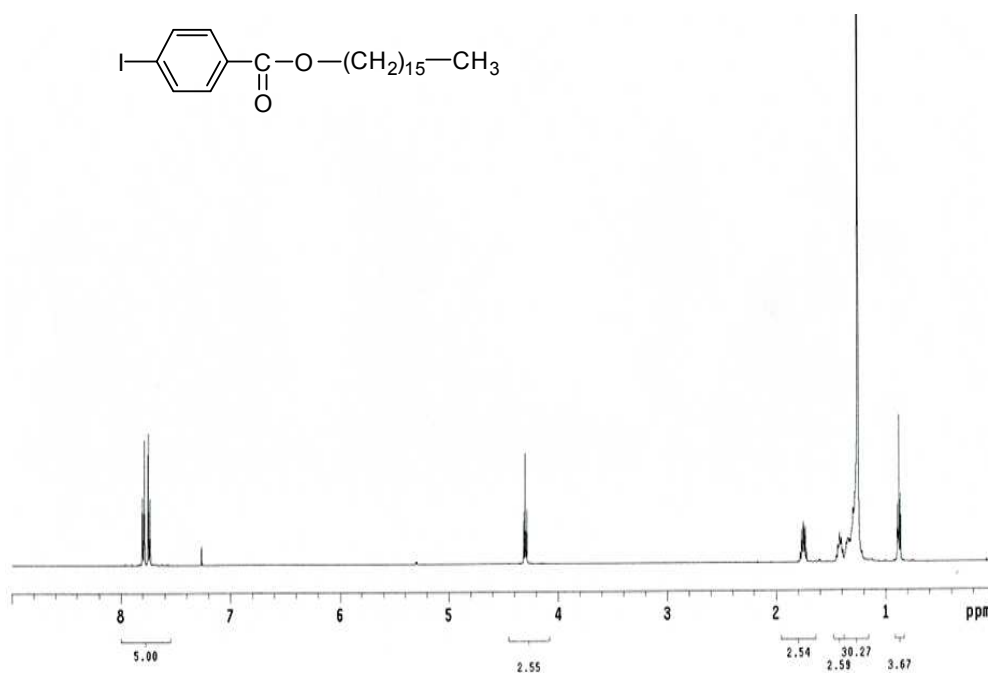


Figure S1. ¹H-N.M.R. spectra (500 MHz) in CDCl₃ of hexadecyl-4-iodobenzoate.

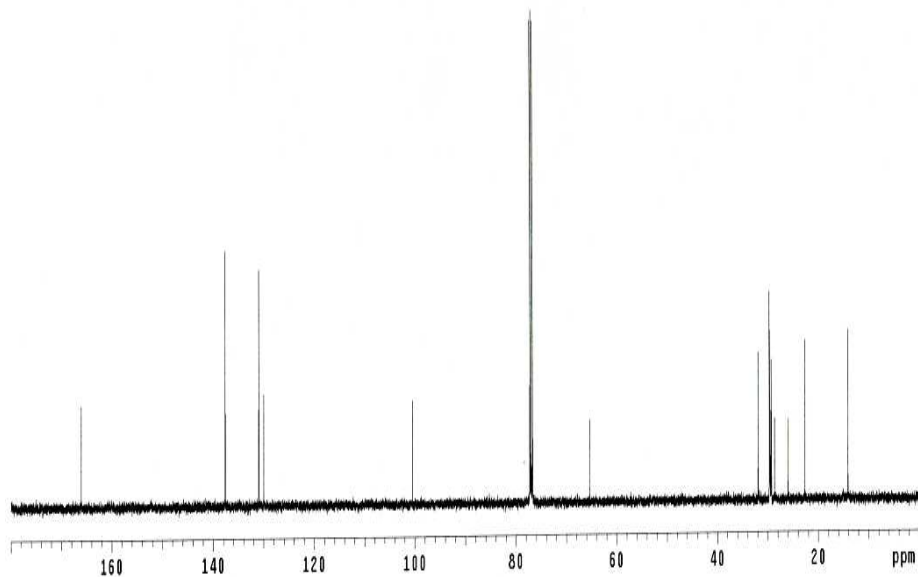


Figure S2. ^{13}C -N.M.R spectra (125 MHz) in CDCl_3 of hexadecyl-4-iodobenzoate.

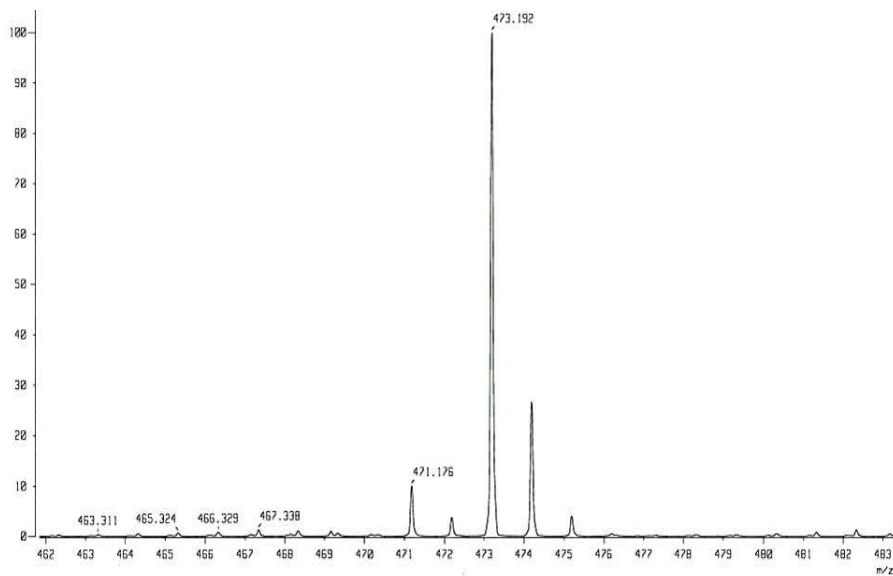


Figure S3. Mass spectra of hexadecyl-4-iodobenzoate.

Synthesis of hexadecyl-4-tributylstannylbenzoate: Hexabutylditin (0.78 ml, 0.9 g, 1.55 mmol) and the catalytic amount of tetrakis(triphenylphosphine)palladium (22.42 mg, 19.4 μ mol) were added to a stirred solution of hexadecyl-4-iodobenzoate (0.46 g, 0.97 mmol) in anhydrous toluene (20ml). The reaction mixture was refluxed for 8 h until the solution turned black. After cooling, the toluene was evaporated from reaction mixture under reduced pressure. The resulting black oil was purified via column chromatography on silica, eluting with hexane/ethyl acetate (20:1) to afford hexadecyl-4-tributylstannylbenzoate as a colorless oil (0.43 g, 71% yield). ^1H NMR (500 MHz, CDCl_3): δ 0.88-0.91 (m, 12H), 1.02 -1.16 (m, 6H), 1.21-1.39 (m, 30H), 1.42-1.62 (m, 8H), 1.74-1.79 (m, 2H), 4.30-4.33 (t, 2H, $J = 6.5$ Hz), 7.55-7.57 (dd, 2H, $J = 8$ Hz), 7.96-7.98 (dd, 2H, $J = 8$ Hz); ^{13}C NMR (125 MHz, CDCl_3): δ 9.63, 13.63, 14.10, 22.69, 26.06, 27.31, 28.75, 28.94, 29.02, 29.11, 29.29, 29.36, 29.54, 29.59, 29.64, 29.66, 29.67, 29.69, 31.92, 64.97, 128.34, 129.96, 136.35, 149.39, 167.08; HRMS (FAB) calculated for $\text{C}_{35}\text{H}_{65}\text{O}_2\text{Sn}$, 637.4007 $[(\text{M}+\text{H})^+]$, found: 637.4003 $[(\text{M}+\text{H})^+]$.

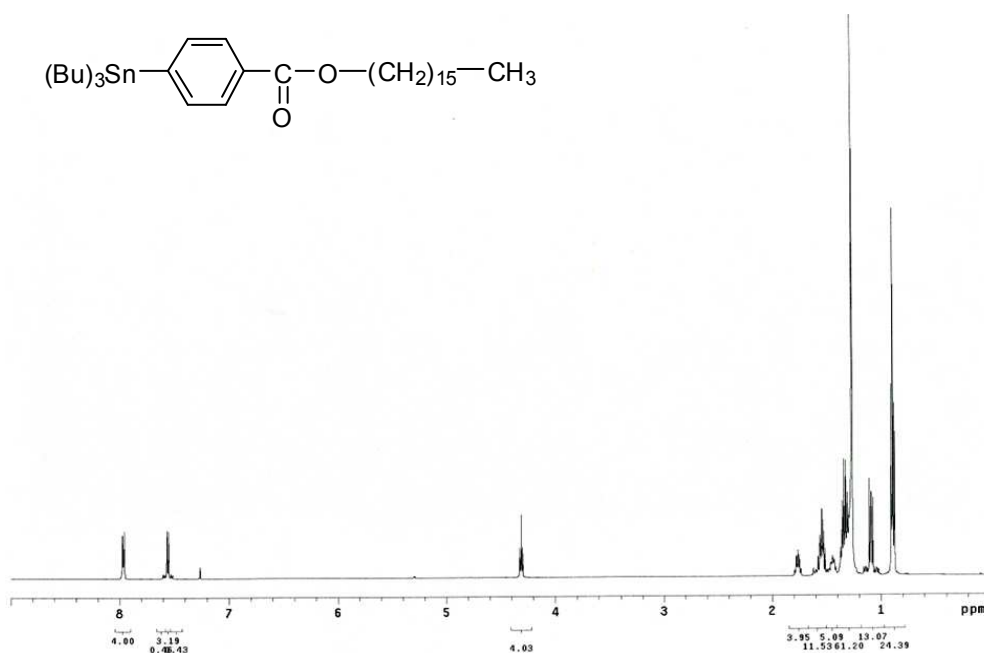


Figure S4. ^1H -N.M.R spectra (500 MHz) in CDCl_3 of hexadecyl-4-tributylstannylbenzoate.

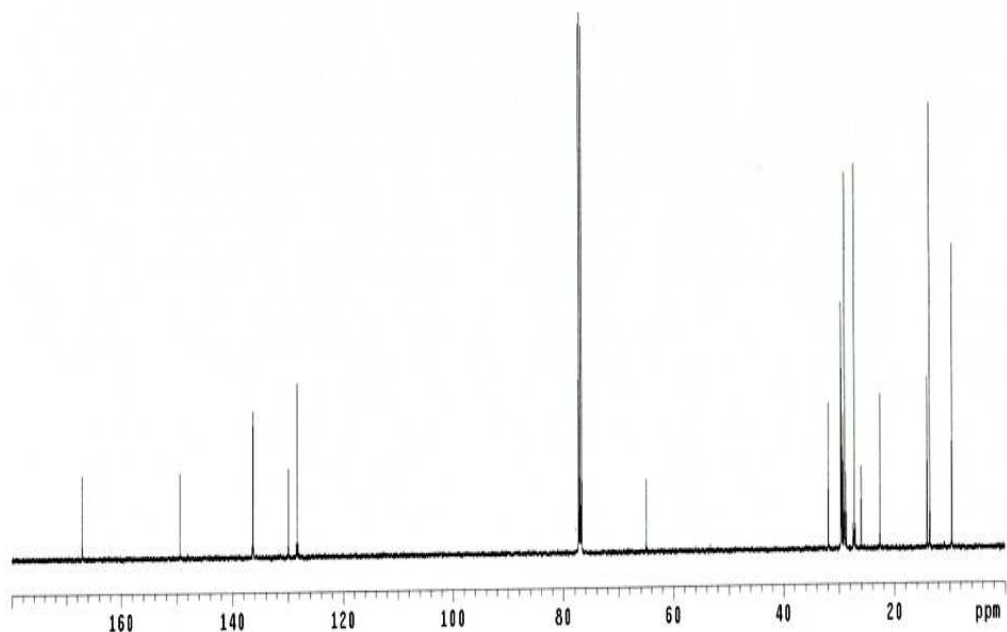


Figure S5. ^{13}C -N.M.R spectra (125 MHz) in CDCl_3 of hexadecyl-4-tributylstannylbenzoate.

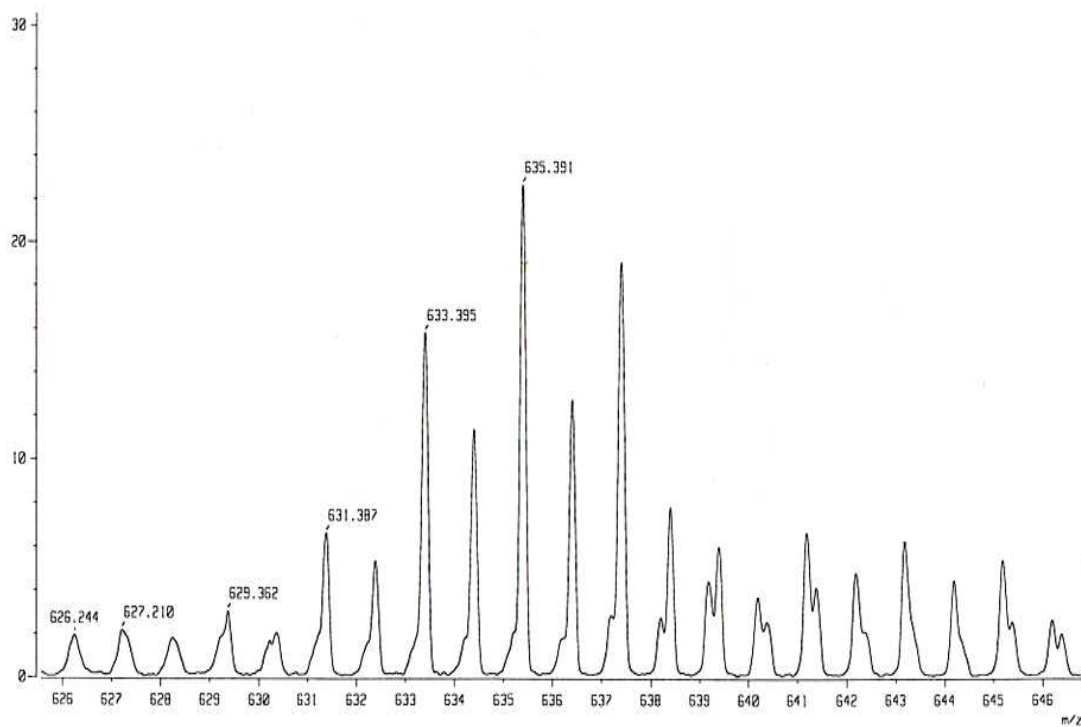


Figure S6. Mass spectra of hexadecyl-4-tributylstannylbenzoate.

Radiolabeling of HIB: To a mixture of HIB precursor (hexadecyl-4-tributylstannylbenzoate, 100 µg) in 100 µl of acetic acid, 100 µl of 1 N HCl, 100 µl of 3% H₂O₂ and Na¹²⁴I (0.5 - 5 mCi) was added. The mixture was reacted for 30 min at 70°C and then the reaction was ended by addition of 100 µl of NaHSO₃. This reaction was monitored by silica-TLC using mobile phase (hexane:ethyl acetate (20:1 v/v); Retention factor: free ¹²⁴I ions = 0.0, [¹²⁴I]HIB = 0.45. After removing the solvent under vacuum at 50 °C, the isolated [¹²⁴I]HIB dissolved in acetonitrile, then supernatant centrifuged at 8000 g for 5 min. After removing the solvent under vacuum at 50°C, the isolated [¹²⁴I]HIB was dissolved in dichloromethane. Radiochemical yield was analyzed by AR-2000 radio-TLC Imaging Scanner (Bioscan, Washington, D.C., USA).

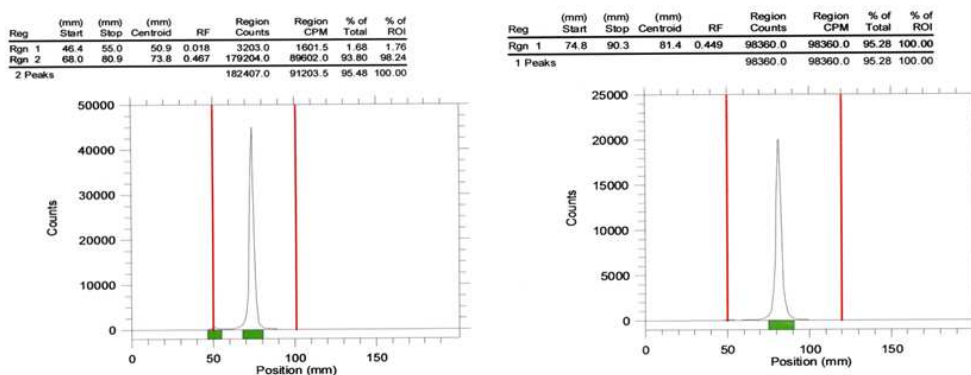


Figure S7. Radio-TLC chromatogram of [¹²⁴I]HIB (left: after radiolabeling, right: after purification).

Preparation of [¹²⁴I]HIB-Gd-containing liposome: Gd-DTPA containing liposomes were prepared with 1,2-dipalmitoyl-sn-glycero-3-phosphocholine (DPPC; 1 mg, 1.36 μmol), 1,2-dihexadecanoylsn-glycero-3-phospho-(1'-rac-glycerol) (DPPG; 1 mg, 1.34 μmol), cholesterol (0.4 mg, 1.0 μmol), 1,2-distearoyl-sn-glycero-3-phosphoethanolamine-N[methoxy(polyethyleneglycol)-2000] ammonium salt (DSPE-PEG2000; 1.8 mg, 0.68 μmol) and 1,2-dipalmitoyl-sn-glycero-3-phosphoethanolamine-N-diethylenetriaminopentaacetic acid (Gd-DTPA-DPPE; 3 mg, 2.3 μmol). The lipids in chloroform were well mixed with the pre-synthesized [¹²⁴I]HIB (0.5 - 3 mCi) in a round flask, and dried by a rotary evaporator to make a lipid thin film, which was hydrated with saline (1 mL) by the incubation for 25 min at 50 °C. The formed opaque liposomal solution was sequentially extruded through nuclepore polycarbonate membrane filters (Whatman, Kent, UK) with 1000, 400, 200, 100-nm pore sizes (9 passes for 1 μm and 400 nm; and 15 passes for 200 nm; and 21 passes for 100 nm pore size) at 55 °C (Avanti's mini-extruder, Avanti Polar lipids, AL, USA). The extruded liposomes were purified by a gel chromatography on PD-10 column (GE Healthcare, Pittsburgh, USA) with saline as an eluent.

Physicochemical characterization of [¹²⁴I]HIB-Gd-containing liposome: The particle size of the liposomes was measured by light scattering with a particle size analyzer (ELS-Z, Zeta potential and particle size analyzer, Otsuka, Japan). Size and surface morphology of liposomes were observed using transmission electron microscopy (TEM, HITACHI, Tokyo, Japna). The liposomes were loaded on the surface of copper grid with carbon film and stained with 2% uranyl acetate for 5 min. The concentration of Gd(III) ions in the liposomes was measured using an Inductively Coupled Plasma-Spectrophotometer (PerkinElmer).

In vitro imaging study of [¹²⁴I]HIB-Gd-containing liposome: Each 200 μ L aliquot from size exclusion column was collected in 96 well, and serially imaged using optical, PET and MR imaging. MicroPET image was acquired by small-animal Inveon PET scanner (Siemens) for 20 min scan time using ASIPro software (detector pixel spacing = 1.6 mm \times 1.6 mm; field of view (FOV) = 10 cm transaxial \times 12.7 cm axial; detector crystal array = 20 \times 20; energy window of 350–650 keV). Optical image was acquired by IVIS spectrum (PerkinElmer) for 1 min exposure time using Living Image software (block excitation; open emission filter; field of view (FOV) = D (22.5 \times 22.5 cm); Bin = 8; f = 1; exposure time = 60 s). The quantification was based on photon radiance (p/sec/cm³/sr). Finally, MR image was performed using GE Excite 1.5T scanner (repetition time (TR) = 300 ms; echo time (TE) = 13 ms; field of view (FOV) = 8 cm; image matrix=192 \times 128; 1.0 mm slice thickness; number of acquisition (NEX) = 8).

Determination of Partition Coefficients: The $\log P$ values of [¹²⁴I]HIB were determined by adding 5 μ L of the labeled complex (\sim 40-50 μ Ci) to a mixture of 500 μ L of 1-octanol and 500 μ L of water. The resulting solutions were vigorously vortexed for 5 min at room temperature, then centrifuged for 5 min to ensure complete separation of layers. From each of the six sets, 100 μ L aliquot was removed from each phase into screw tubes and counted separately in a gamma counter. The partition coefficient was calculated as a ratio of counts in the 1-octanol fraction to counts in the water fraction. The $\log P$ values were reported in an average of six measurements.

Blood half-life measurement of [¹²⁴I]HIB and [¹²⁴I]HIB-labeled liposome: To determine the blood half-life of [¹²⁴I]HIB-assembled liposome and [¹²⁴I]HIB, female BALB/C mice were tail intravenous injected with ~17 uCi of [¹²⁴I]HIB-assembled liposome and [¹²⁴I]HIB in 200mL of saline. Blood samples were serially collected from the retro-orbital sinus. At the desired time points, ca. 50- μ l volume of blood was obtained and kept in pre-weighed heparinized capillaries tube (Fisher Scientific, New Hampshire, USA). Then, the blood samples were weighed and counted using WIZARD² Automatic Gamma Counter (PerkinElmer).

Both blood half-life data of [¹²⁴I]HIB and [¹²⁴I]HIB-assembled liposome fit a two-phase exponential decay model (GraphPad Prism 5.0, San Diego, USA). The blood retention of [¹²⁴I]HIB-assembled liposome was 28.7% of injected dose per gram (%ID/g) at 15 min and slowly decreased to 3.4%ID/g at 6 h after injection, while [¹²⁴I]HIB cleared quickly from blood with only 2.9%ID/g left in blood at 15 min post-injection.

Animal study: All animal experiments were conducted in compliance with the Animal Care and Use Committee requirements of Kyungpook National University. CT26 cells (murine colon cancer) were cultured in DMEM (Dulbecco's Modified Eagle's Medium) containing high glucose supplemented with 10% fetal bovine serum (FBS) and 1% penicillin-streptomycin. Female BALB/c mice at 6 weeks of age were obtained from Hyochang science (Daegu, Korea). The mice were injected subcutaneously in the right femoral region with 5×10^6 CT26 cells suspended in 200 μ l DMEM containing high glucose. When the tumors reached 7 – 12 mm in diameter (10 – 14 days after implantation), the mice were used for multimodal imaging experiments. Mice were anesthetized with 1-2% isoflurane in 100% O₂ during injection and imaging acquisition.

In vivo Optical imaging: All optical images were measured from a bioluminescence channel with no excitation light or emission filters using IVIS spectrum (Caliper Life Sciences, Inc., USA). The optical image was thresholded to maximize the visualization of the region of interest and to minimize background. The imaging parameters were as follows: block excitation; open emission filter; field of view (FOV) = D (22.5 \times 22.5 cm); Bin = 8; $f = 1$; exposure time = 120 s. The quantification was based on photon radiance (p/sec/cm³/sr).

In vivo microPET imaging: PET scans were performed using a small-animal Inveon PET scanner (Siemens, Knoxville, TN, USA). Mice were fixed in prone position on the bed. All microPET images were reconstructed by a 2-dimensional ordered-subsets expectation maximum (OSEM) algorithm and focal accumulations on microPET images were quantified by region of interest (ROI) analysis. Tumor-to-organ ratios were calculated using average counts per voxel on coronal images. The imaging parameters were as follows: detector pixel spacing = 1.6 mm \times 1.6 mm; field of view (FOV) = 10 cm transaxial \times 12.7 cm axial; detector crystal array = 20 \times 20; energy window of 350 – 650 keV.

In vivo MR imaging: Whole body MR images were taken with a 1.5 T MR unit (GE Healthcare, Milwaukee, WI, USA) equipped with a home-made small animal RF coil. The coil was of the receiver type with its inner diameter being 50 mm. The imaging parameters for SE (Spin Echo) were the following: repetition time (TR) = 300 ms; echo time (TE) = 13 ms; field of view (FOV) = 8 cm; image matrix = 192 × 128; 1.0 mm slice thickness; number of acquisition (NEX) = 8.

MR Image analysis: The anatomical locations with enhanced contrast were identified with respect to liver and tumor on post-contrast MR images. For quantitative measurement, signal intensities in specific regions of interest (ROI) measured using Image J (National Institutes of Health, USA). The CNR (Contrast to Noise Ratio) was calculated using below equation, where SNR is the signal to noise ratio.

$$\text{CNR} = (\text{SNR}_{\text{post}} - \text{SNR}_{\text{pre}})$$

Figure S8 shows rapid increase of contrast-to-noise ratio (CNR) up to 30 min and slowly increased to maximum value at 3 h in both liver and tumor. But, the CNR values in liver and tumor were gradually decreased afterward.

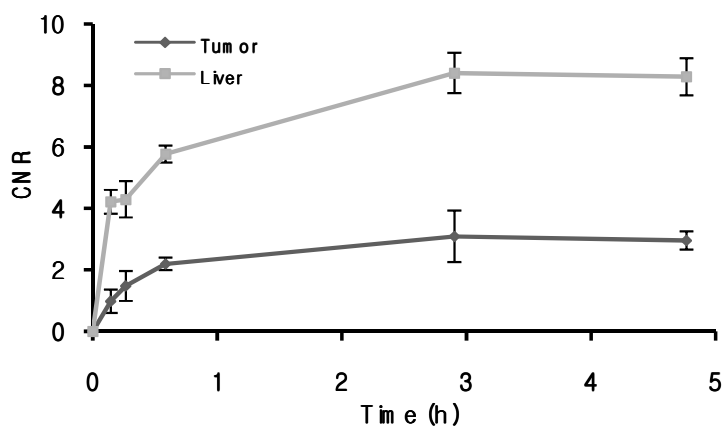


Figure S8. CNR (Contrast to Noise Ratio) profiles of tumor and liver after liposome injection into tumor models.